



# The nature of O<sub>2</sub> activation by the ethylene-forming enzyme 1-aminocyclopropane-1-carboxylic acid oxidase

Liviu M. Mirica and Judith P. Klinman\*

Departments of Chemistry and Molecular and Cell Biology, University of California, Berkeley, CA 94720

Contributed by Judith P. Klinman, December 10, 2007 (sent for review November 15, 2007)

Ethylene is a plant hormone important in many aspects of plant growth and development such as germination, fruit ripening, and senescence. 1-Aminocyclopropane-1-carboxylic acid (ACC) oxidase (ACCO), an O<sub>2</sub>-activating ascorbate-dependent nonheme iron enzyme, catalyzes the last step in ethylene biosynthesis. The O<sub>2</sub> activation process by ACCO was investigated using steady-state kinetics, solvent isotope effects (SIEs), and competitive oxygen kinetic isotope effects (<sup>18</sup>O KIEs) to provide insights into the nature of the activated oxygen species formed at the active-site iron center and its dependence on ascorbic acid. The observed large <sup>18</sup>O KIE of 1.0215 ± 0.0005 strongly supports a rate-determining step formation of an Fe<sup>IV</sup>=O species, which acts as the reactive intermediate in substrate oxidation. The large SIE on *k*<sub>cat</sub>/*K*<sub>m</sub>(O<sub>2</sub>) of 5.0 ± 0.9 suggests that formation of this Fe<sup>IV</sup>=O species is linked to a rate-limiting proton or hydrogen atom transfer step. Based on the observed decrease in SIE and <sup>18</sup>O KIE values for ACCO at limiting ascorbate concentrations, ascorbate is proposed to bind in a random manner, depending on its concentration. We conclude that ascorbate is not essential for initial O<sub>2</sub> binding and activation but is required for rapid Fe<sup>IV</sup>=O formation under catalytic turnover. Similar studies can be performed for other nonheme iron enzymes, with the <sup>18</sup>O KIEs providing a kinetic probe into the chemical nature of Fe/O<sub>2</sub> intermediates formed in the first irreversible step of the O<sub>2</sub> activation.

2 His, 1-Asp proteins | high-valent iron oxo species | oxygen-18 kinetic isotope effects | nonheme iron enzymes

Ethylene is a major plant hormone important in many aspects of plant growth and development such as germination, fruit ripening, and senescence (1). The ability to control ethylene formation in a time-dependent manner would have far-reaching economic, agricultural, and environmental implications. The last step in the biosynthesis of ethylene, the two electron oxidation of 1-aminocyclopropane-1-carboxylic acid (ACC) to ethylene, CO<sub>2</sub>, and HCN, is catalyzed by ACC oxidase (ACCO) (2–4). This reaction also requires the concomitant reduction of O<sub>2</sub> to water and the oxidation of ascorbate to dehydroascorbate (Fig. 1), whereas CO<sub>2</sub> (or bicarbonate) has been shown to act as an activator for ethylene formation (5).

ACCO belongs to the family of O<sub>2</sub>-activating nonheme iron enzymes. Although the sequence homology among these enzymes is not high, all their active sites contain a single ferrous iron bound in a tridentate ligand arrangement referred to as a “2-His-1-carboxylate facial triad” (4). A crystal structure of ACCO has been reported (6), revealing a solvent-exposed active site and confirming the ligation of the iron center (His-177, Asp-179, and His-234) inferred from mutagenesis studies (7), and the general jellyroll motif found in other nonheme iron enzymes (8, 9).

What distinguishes ACCO from the other enzymes of this family is the two-electron donating cosubstrate needed for reducing O<sub>2</sub> to water: ascorbate in the case of ACCO (10–13) and α-ketoglutarate (αKG) in almost all other known examples (4). The mechanism of αKG-dependent enzymes has been

studied extensively, and it generally is accepted that O<sub>2</sub> activation at the iron center is linked to oxidative decarboxylation of the αKG, ultimately forming an Fe<sup>IV</sup>=O species as the reactive intermediate (14–17). This high-valent Fe/O<sub>2</sub> species functions as a “generic” oxidant for a wide range of oxidation/oxygenation reactions.

In contrast to the αKG-dependent enzymes, where αKG rather than substrate binds to the metal center, spectroscopic studies of ACCO have shown that ACC coordinates to the iron center via both its amino and carboxylate groups (10, 18).<sup>†</sup> This finding implies a distinctly different mode for reductant interaction with ACCO than for most other nonheme iron enzymes. Magnetic circular dichroism (MCD) studies indicate that the active-site iron center is six-coordinate in the resting state Fe(II)-ACCO (19). On addition of ACC and ascorbate, the iron center becomes five-coordinate, allowing for O<sub>2</sub> binding and activation. These results are in line with steady-state kinetic analyses that suggest an ordered process where ACC binding to ACCO must precede O<sub>2</sub> binding, although it could not be distinguished whether ascorbate binds before ACC or after O<sub>2</sub> (12).

Single-turnover experiments showed that a substoichiometric amount of ethylene was formed in the absence of ascorbate, with the presence of either CO<sub>2</sub> or bicarbonate being essential for enzyme turnover (13). Although ascorbate was proposed to act mainly as a reductant for restoring the iron to the ferrous state, the rate of ethylene formation under single-turnover conditions was significantly lower than under steady-state conditions, suggesting that ascorbate is needed for O<sub>2</sub> activation under catalytic turnover (Fig. 2).

From these accumulated results, it is clear that the complexity of the ACCO chemistry presents a challenge for mechanistic enzymologists and requires further examination. In this study, steady-state kinetics, solvent isotope effects (SIEs), and competitive oxygen kinetic isotope effects (<sup>18</sup>O KIEs) are used to provide insights into the rate-limiting steps contributing to the interaction of O<sub>2</sub> with ACCO, the nature of the Fe/O<sub>2</sub> intermediates, and the role of ascorbate in O<sub>2</sub> activation. Of particular interest is the investigation of the Fe<sup>IV</sup>=O species formation and its proposed role in substrate oxidation (20).

## Results

**SIEs on Steady-State Parameters.** The kinetic parameters for ACCO have been measured by monitoring the amount of O<sub>2</sub> consumed by using a Clark electrode. The obtained kinetic

Author contributions: L.M.M. and J.P.K. designed research; L.M.M. performed research; and L.M.M. and J.P.K. wrote the paper.

The authors declare no conflict of interest.

Freely available online through the PNAS open access option.

\*To whom correspondence should be addressed. E-mail: klinman@berkeley.edu.

<sup>†</sup>It also was shown that ACC and O<sub>2</sub> could bind simultaneously to the iron, with ascorbate proposed to bind to the enzyme for efficient electron transfer (10, 13).

© 2008 by The National Academy of Sciences of the USA

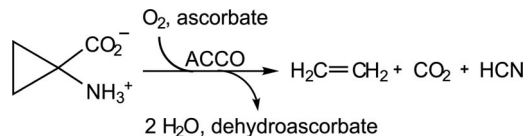


Fig. 1. The reaction catalyzed by ACCO.

parameters [ $k_{\text{cat}} = 36.7 \pm 1.1 \text{ min}^{-1}$ ,  $K_{\text{m}}(\text{ACC}) = 92 \pm 10 \mu\text{M}$ ,  $K_{\text{m}}(\text{Asc}) = 5.5 \pm 0.7 \text{ mM}$ ,  $K_{\text{m}}(\text{O}_2) = 67 \pm 6 \mu\text{M}$ ] are similar to our previous results (12). Because both ACC and ascorbate have solvent-exchangeable protons, the only deuterium isotope effects that can be measured are kinetic SIEs. Comparison of the kinetic parameters measured in both  $\text{H}_2\text{O}$  and  $\text{D}_2\text{O}$  revealed the presence of SIEs (Table 1). The measured values for  $^{\text{D}_2\text{O}}k_{\text{cat}}$ ,  $^{\text{D}_2\text{O}}k_{\text{cat}}/K_{\text{m}}(\text{ACC})$ , and  $^{\text{D}_2\text{O}}k_{\text{cat}}/K_{\text{m}}(\text{Asc})$  are  $\approx 2.3$ , identical within experimental error, suggesting changes in hydrogen bonding between the reactants and the transition state. None of the kinetic parameters has been found to vary between pH 6 and 8 (data not shown), indicating the lack of a  $\text{pK}_a$  effect as the origin of the SIEs. Interestingly, the  $^{\text{D}_2\text{O}}k_{\text{cat}}/K_{\text{m}}(\text{O}_2)$  value is  $5.0 \pm 0.9$  (Table 1 and Fig. 3), an uncommonly large value for a SIE. Such a value suggests that the rate-determining step in  $\text{O}_2$  activation involves either a proton-coupled electron transfer (PCET) or hydrogen atom transfer (HAT), as discussed below.

**$^{18}\text{O}$  KIE.** The  $^{18}\text{O}$  KIE on  $k_{\text{cat}}/K_{\text{m}}(\text{O}_2)$ ,  $^{18}k_{\text{cat}}/K_{\text{m}}(\text{O}_2)$ , was measured for ACCO to determine the extent of change in oxygen bond order in the steps leading up to the first irreversible step in  $\text{O}_2$  activation. Competitive  $^{18}\text{O}$  KIEs were determined from the fractionation of oxygen isotopes, i.e., the change in the  $^{18}\text{O}/^{16}\text{O}$  ratio during the consumption of  $\text{O}_2$  catalyzed by ACCO (21). The fractional conversions used for these measurements were between 15% and 70%. The isotope fractionation plot ( $^{18}\text{O}/^{16}\text{O}$  isotopic ratios of ratios versus fractional conversion) for ACCO is shown in Fig. 4A. The  $^{18}\text{O}$  KIEs were obtained by fitting the data to Eq. 1, where  $R_f$  is the  $^{18}\text{O}/^{16}\text{O}$  isotopic ratio at  $f$  fractional conversion and  $R_0$  is the isotopic ratio before the enzymatic reaction.

$$\frac{R_f}{R_0} = (1 - f)^{1/[(^{18}\text{O KIE}) - 1]} \quad [1]$$

The data are well fitted by Eq. 1 to give an  $^{18}\text{O}$  KIE value of  $1.0215 \pm 0.0005$ . This observed  $^{18}\text{O}$  KIE is among the largest for  $\text{O}_2$ -activating metalloenzymes (22), suggesting a significant change in the oxygen bond order, attributable to formation of a

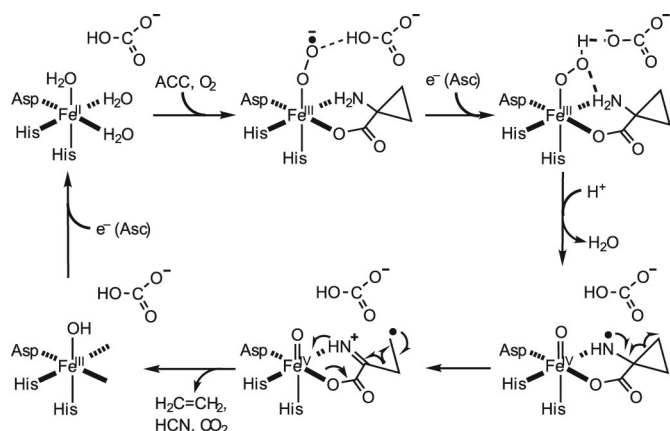


Fig. 2. Previously proposed catalytic mechanism for ACCO (13). Asc, ascorbate.

high-valent  $\text{Fe}^{\text{IV}}=\text{O}$  species in the first irreversible step (see below). The measured  $^{18}\text{O}$  KIE for the much slower background  $\text{O}_2$  consumption caused by ascorbate and iron in the absence of enzyme is  $1.0111 \pm 0.0002$  (data not shown), excluding an artificial inflation of the ACCO  $^{18}\text{O}$  KIE value from the non-enzymatic reactions.

**SIE on  $^{18}\text{O}$  KIE.** To test the role of protons during  $\text{O}_2$  activation, the  $^{18}\text{O}$  KIE also was measured in  $\text{D}_2\text{O}$ . Because of lower activity of ACCO in  $\text{D}_2\text{O}$ , data points for the ACCO reaction were collected only for fractional conversions between 10% and 30%. The measured  $^{18}\text{O}$  KIE for ACCO in  $\text{D}_2\text{O}$  is  $1.0209 \pm 0.0004$  (Fig. 4A). This value is within experimental error of the  $^{18}\text{O}$  KIE in  $\text{H}_2\text{O}$ . The lack of a SIE on the  $^{18}\text{O}$  KIE of ACCO indicates that solvent deuteration does not impact the relative activation barriers of the steps leading up to and including the first irreversible step of  $k_{\text{cat}}/K_{\text{m}}(\text{O}_2)$ .

**Ascorbate Effect on SIE and  $^{18}\text{O}$  KIE.** Ascorbate is an essential substrate for ACCO and acts as a reductant to fully reduce  $\text{O}_2$  to water. Its role in ACCO activity was tested by measuring the kinetic parameters at lower ascorbate concentration (2 mM, 35% of its  $K_{\text{m}}$  value). Because of lower activity of ACCO at this ascorbate concentration, data points were collected only for fractional conversions between 10% and 30%. Measurement of the  $^{18}\text{O}$  KIE for ACCO under these conditions reveals a value of  $1.0157 \pm 0.0004$  (Fig. 4B), lower than the value obtained under saturating ascorbate concentration ( $1.0215 \pm 0.0005$ ).

In addition, the SIEs measured at 2 mM ascorbate show that the apparent  $^{\text{D}_2\text{O}}k_{\text{cat}}/K_{\text{m}}(\text{O}_2)$  value decreases to  $2.7 \pm 0.7$ , within experimental error of the SIEs of  $\approx 2.3$  for the other kinetic parameters that do not change with ascorbate concentration (Table 1). The decrease in both  $^{18}\text{O}$  KIE and  $^{\text{D}_2\text{O}}k_{\text{cat}}/K_{\text{m}}(\text{O}_2)$  values at lower ascorbate concentrations is not expected for an ordered terreactant enzymatic reaction, suggesting a possible change in the order of ascorbate binding to ACCO that has an effect on the  $\text{O}_2$  activation steps (see below).

## Discussion

The gene for the tomato ACCO has been expressed recently in this laboratory in high yield in *E. coli* and purified to homogeneity to yield a protein with approximately 10 times greater activity than previously reported (12). Some of the initial studies undertaken with this enzyme have included the kinetic order for binding of all substrates to enzyme, the relationship of  $\text{O}_2$  activation to substrate activation, and the chemical steps that lead from ACC to its products. Steady-state kinetic studies indicated a sequential mechanism involving a quaternary complex (ACCO, ACC,  $\text{O}_2$ , and ascorbate) and an equilibrium-ordered pattern with ACC binding before  $\text{O}_2$  but were unable to distinguish whether ascorbate binds before ACC or after  $\text{O}_2$  (12).

Activation of ACC by ACCO is likely to occur by one-electron oxidation or hydrogen atom abstraction from the amine group to form an amine radical cation or aminyl radical, respectively (23). Rapid radical rearrangement results in cleavage of the cyclopropane ring and eventually formation of ethylene, HCN, and  $\text{CO}_2$ . In a recent study, the behavior of three cyclic and three acyclic substrate analogs was analyzed in regard to turnover rates, product distribution, and  $\text{O}_2$  uncoupling (20). Although these analogs have different structures, the turnover rates ( $k_{\text{cat}}$ ) are within a factor of four of ACC, suggesting that the rate-determining step occurs before substrate oxidation (20). It also was proposed that the first committed step involved the formation of an  $\text{Fe}^{\text{IV}}=\text{O}$  species, which acts as the oxidant in substrate activation. An  $\text{Fe}^{\text{IV}}=\text{O}$  species had been implicated previously as the oxidant that activates the substrate in the  $\alpha\text{KG}$ -dependent enzymes (14–16). However, as noted ACCO uses ascorbate as the reductant, which can serve as a one- or two-electron donor;

**Table 1. Kinetic parameters for ACCO in H<sub>2</sub>O and D<sub>2</sub>O**

Parameter	20 mM ascorbate*			2 mM ascorbate†		
	H <sub>2</sub> O	D <sub>2</sub> O	SIE	H <sub>2</sub> O	D <sub>2</sub> O	SIE
$k_{cat}$ , min <sup>-1</sup> *	36.7 ± 1.1	17.5 ± 1.2	2.1 ± 0.2	13.4 ± 0.9 <sup>§</sup>	5.68 ± 0.54 <sup>§</sup>	2.3 ± 0.3
$k_{cat}/K_m(O_2)$ , <sup>‡</sup> μM <sup>-1</sup> ·min <sup>-1</sup>	0.547 ± 0.06	0.109 ± 0.017	5.0 ± 0.9	0.114 ± 0.018 <sup>§</sup>	0.042 ± 0.008 <sup>§</sup>	2.7 ± 0.7
$k_{cat}/K_m(ACC)$ , <sup>¶</sup> μM <sup>-1</sup> ·min <sup>-1</sup>	0.280 ± 0.045	0.117 ± 0.015	2.4 ± 0.5	0.069 ± 0.011 <sup>§</sup>	0.030 ± 0.005 <sup>§</sup>	2.3 ± 0.5
$k_{cat}/K_m(Asc)$ , <sup>  </sup> mM <sup>-1</sup> ·min <sup>-1</sup>	5.68 ± 0.60	2.32 ± 0.49	2.4 ± 0.6	N/A	N/A	N/A

\*Saturating conditions: 1 mM ACC, 258 μM O<sub>2</sub>, 20 mM ascorbate, and 20 mM NaHCO<sub>3</sub>, 25°C, pH 7.2.

†Saturating conditions in all substrates except for the varied substrate and fixed 2 mM ascorbate.

‡Varied O<sub>2</sub> concentration and 1 mM ACC, 20 mM ascorbate, and 20 mM NaHCO<sub>3</sub>.

§Apparent  $k_{cat}$ ,  $k_{cat}/K_m(O_2)$ , and  $k_{cat}/K_m(ACC)$ .

¶Varied ACC concentration and 258 μM O<sub>2</sub>, 20 mM ascorbate, and 20 mM NaHCO<sub>3</sub>.

||Varied ascorbate concentration and 1 mM ACC, 258 μM O<sub>2</sub>, and 20 mM NaHCO<sub>3</sub>.

Lipscomb, Que, and colleagues suggested that ACC oxidation may involve either direct HAT to an Fe<sup>III</sup>—OOH or prior O—O bond heterolysis to generate Fe<sup>V</sup>=O as the oxidizing species (13). In their examples, an Fe<sup>IV</sup>=O species would be formed concomitant with substrate activation. Although multiple species (Fe<sup>III</sup>—OOH, Fe<sup>IV</sup>=O, or Fe<sup>V</sup>=O) have been discussed as possible oxidants in the context of the ACCO mechanism (13, 20), direct evidence for the catalytic intermediate has been lacking.

**SIE.** The kinetic parameters for ACCO measured in both H<sub>2</sub>O and D<sub>2</sub>O show the presence of SIEs. <sup>D2O</sup> $k_{cat}$ , <sup>D2O</sup> $k_{cat}/K_m(ACC)$ , and <sup>D2O</sup> $k_{cat}/K_m(Asc)$  are identical within experimental error, with values ≈2.3 (Table 1). These SIEs are suggestive of proton transfers occurring along hydrogen bonds involved in general acid/base catalytic stabilization of the transition state (24). However, given the large number of protons in the active site that can exchange with solvent (water molecules coordinated to the iron center, amine protons of ACC, acidic protons of ascorbate, bicarbonate), these SIEs may represent the product of multiple effects and are referred to as background SIEs. A pK<sub>a</sub> origin of the SIE can be eliminated because all kinetic parameters are found to be invariant between pH 6 and 8. Interestingly, <sup>D2O</sup> $k_{cat}/K_m(O_2)$  is 5.0 ± 0.9 (Table 1 and Fig. 3). Such a large SIE indicates that either a PCET or HAT from a solvent-exchangeable site occurs in the rate-limiting step of  $k_{cat}/K_m(O_2)$  (24). Possible proton sources for a PCET process may include

acidic side-chain residues, ascorbate, or bicarbonate, whereas a hydrogen atom may be removed from ascorbate or the ACC amine group.

**<sup>18</sup>O KIE.** In recent years, a number of studies have addressed the early steps in O<sub>2</sub> activation for a series of enzymes, with measurement of competitive <sup>18</sup>O KIEs on  $k_{cat}/K_m(O_2)$  being an important factor in determining the nature of the first commit-

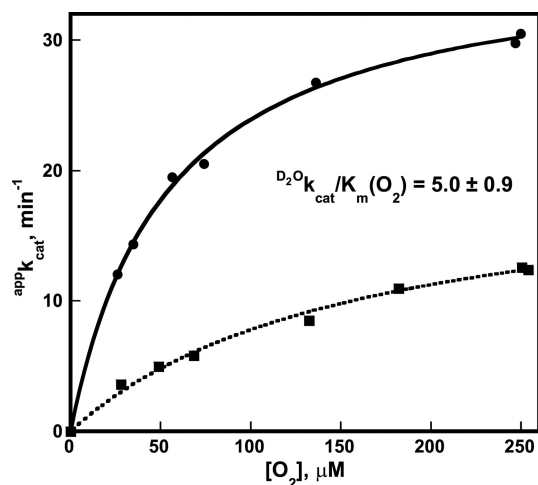


**Fig. 3.** Michaelis–Menten plot for ACCO with O<sub>2</sub> as varied substrate, in H<sub>2</sub>O (●) and D<sub>2</sub>O (■). Conditions: 0.5 μM ACCO, 1 mM ACC, 20 mM ascorbate, and 20 mM NaHCO<sub>3</sub>, 25°C, pH 7.2. The solid and dashed lines are fits to the Michaelis–Menten equation.

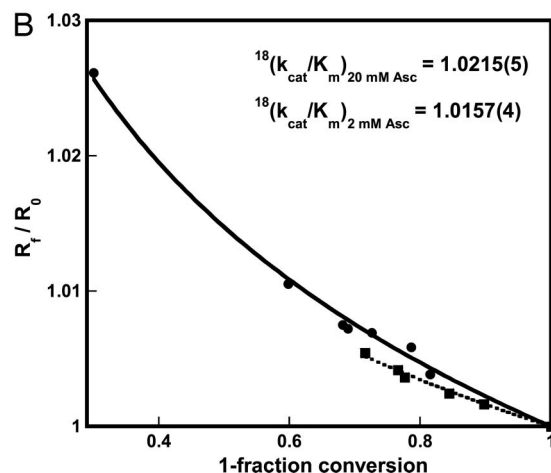
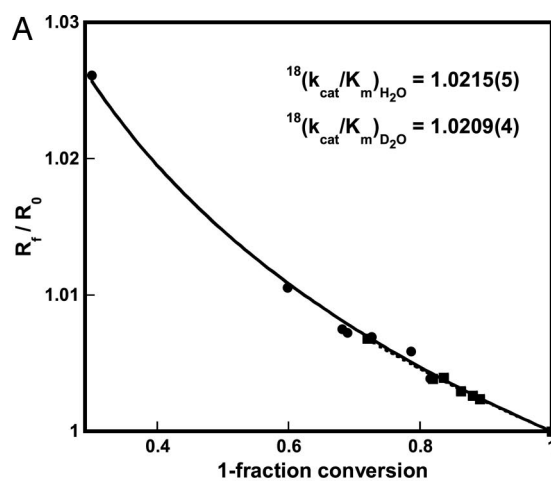


**Fig. 4.** Isotope fractionation plots for ACCO. (A) In H<sub>2</sub>O (●) and D<sub>2</sub>O (■). Conditions: 3.5–8 μM ACCO, 0.3–0.5 mM O<sub>2</sub>, 3 mM ACC, 20 mM ascorbate, and 20 mM NaHCO<sub>3</sub>, 25°C, pH 7.2. (B) Same conditions as in A for 20 mM (●) and 2 mM ascorbate (■), except for the variation in ascorbate concentration. The solid and dashed lines in A and B are fits to Eq. 1 to obtain the <sup>18</sup>O KIE values.

ted step in O<sub>2</sub> activation (22, 25). <sup>18</sup>O KIEs reflect the extent to which a change in oxygen bond order occurs in all reversible steps up through the first irreversible step. For ACCO, the measured <sup>18</sup>O KIE value is 1.0215 ± 0.0005 (Fig. 4A). This result shows clearly that changes in oxygen bond order are occurring in the rate-determining step of *k*<sub>cat</sub>/*K*<sub>m</sub>(O<sub>2</sub>). When compared with other enzymes, the ACCO <sup>18</sup>O KIE is one of the largest measured values for O<sub>2</sub>-activating metalloenzymes, similar to the values reported for the copper enzymes dopamine β-monooxygenase (DβM) and peptidylglycine α-hydroxylating monooxygenase (PHM) (26, 27).

Equilibrium oxygen isotope effects (<sup>18</sup>O EIEs) can be calculated from vibrational frequencies of reactants and products by using the Bigeleisen–Meyer equation (28). For the formation of the Fe<sup>IV</sup>=O species, the calculated <sup>18</sup>O EIE is 1.0287 (29).<sup>‡</sup> Additionally, <sup>18</sup>O EIEs have been reported for the O<sub>2</sub>-binding iron proteins myoglobin and hemerythrin (21), in which O<sub>2</sub> is reduced at an iron center to an Fe<sup>III</sup>—O<sub>2</sub><sup>•−</sup> and Fe<sup>III</sup>—OOH species, respectively. The respective measured <sup>18</sup>O EIEs are 1.0054 ± 0.0006 and 1.0113 ± 0.0005 (Table 2).

Generally, the <sup>18</sup>O EIE values can be used as upper limits for measured <sup>18</sup>O KIEs based on transition state theory (22, 25). This assumption is based on the approximation that, for inner-sphere electron transfer reactions, the heavy-atom isotope effect contribution from the reaction coordinate frequency is negligible (30), as supported by recent results (31). In our case, the calculated EIE for the formation of an Fe<sup>IV</sup>=O species (1.0287) is the only value larger than the <sup>18</sup>O KIE of ACCO (1.0215 ± 0.0005). Given that the first irreversible step is the last step to be expressed in the <sup>18</sup>O KIE, the present result points toward Fe<sup>IV</sup>=O species formation as the first committed step in O<sub>2</sub> activation by ACCO. As an alternative, and by analogy to DβM and PHM (26, 27), it was conceivable that in ACCO the Fe<sup>III</sup>—O<sub>2</sub><sup>•−</sup> species formed rapidly and reversibly, followed by formation of an Fe<sup>III</sup>—OOH species through an irreversible hydrogen atom abstraction from ascorbate or ACC; the former is favored as the reductant based on steady-state kinetics studies that implicate substrate oxidation occurs after the rate-limiting step in *k*<sub>cat</sub> (20). However, given the small measured <sup>18</sup>O EIEs of 1.0054 ± 0.0006 and 1.0113 ± 0.0005 for conversion of Fe(II) to Fe<sup>III</sup>—O<sub>2</sub><sup>•−</sup> and Fe<sup>III</sup>—OOH in myoglobin/hemoglobin and hemerythrin, respectively (21), together with the expected ease with which ascorbate will be oxidized, it is very difficult to envisage the irreversible Fe<sup>III</sup>—OOH formation as the source of the large observed <sup>18</sup>O KIE. The large <sup>18</sup>O KIEs measured for the Cu<sup>II</sup>—OOH formation in the copper monooxygenases DβM and PHM may be attributed to increased back-bonding interactions between copper and the O<sub>2</sub>-derived moiety (32). Turning to the Fe<sup>V</sup>=O species as a potential intermediate in ACCO (13), the absence of experimental frequency data precludes the estimation of an <sup>18</sup>O EIE. However, it is anticipated that Fe<sup>V</sup>=O would be unstable in the presence of semidehydroascorbate, degrading rapidly to the proposed Fe<sup>IV</sup>=O intermediate.

The presence of a large <sup>D2O</sup>*k*<sub>cat</sub>/*K*<sub>m</sub>(O<sub>2</sub>) prompted the examination of the effect of solvent deuteration on the <sup>18</sup>O KIE, to correlate the proton transfer steps with O<sub>2</sub> activation. The measured <sup>18</sup>O KIE in D<sub>2</sub>O is 1.0209 ± 0.0004, within experimental error of the <sup>18</sup>O KIE in H<sub>2</sub>O (Fig. 4A). The lack of a SIE on the <sup>18</sup>O KIE suggests that solvent deuteration does not impact the relative energies of the transition states for the O<sub>2</sub> activation steps, which implicates Fe<sup>IV</sup>=O species formation through a PCET step that is fully rate-limiting for *k*<sub>cat</sub>/*K*<sub>m</sub>(O<sub>2</sub>).

<sup>‡</sup>A similar value (1.0274) is obtained by taking the square root of the previously calculated <sup>18</sup>O EIE for the formation of an Fe<sup>V</sup>=O species from doubly labeled <sup>18,18</sup>O<sub>2</sub> (29).

**Table 2. Experimental and calculated EIEs for the formation of Fe/O<sub>2</sub> species (21, 29)**

Reaction	<sup>18</sup> O EIE
Fe <sup>II</sup> + O <sub>2</sub> ⇌ Fe <sup>III</sup> —O <sub>2</sub> <sup>•−</sup>	1.0054 (Exp.)*
Fe <sup>II</sup> + O <sub>2</sub> $\xrightleftharpoons[e^-, H^+]{}$ Fe <sup>III</sup> —OOH	1.0113 (Exp.)*
Fe <sup>II</sup> + O <sub>2</sub> $\xrightleftharpoons[2e^-, 2H^+]{}$ Fe <sup>IV</sup> —O + H <sub>2</sub> O	1.0287 (Calc.) <sup>‡</sup>

\*Experimental (Exp.) values measured for myoglobin and hemerythrin, respectively (21).

<sup>‡</sup>A similar result is obtained by taking the square root of the calculated (Calc.) value for the reaction with doubly labeled <sup>18,18</sup>O<sub>2</sub> (29).

**The Role of Ascorbate in O<sub>2</sub> Activation.** Given the ambiguous role of ascorbate during O<sub>2</sub> activation, the impact of ascorbate was investigated by measuring the <sup>18</sup>O KIE at a lower ascorbate concentration (2 mM), below its *K*<sub>m</sub> value. Assuming an ordered terreactant mechanism, if ascorbate binds first, followed by ACC, and O<sub>2</sub> binds last, then *k*<sub>cat</sub>/*K*<sub>m</sub>(O<sub>2</sub>) and consequently the <sup>18</sup>O KIE will be independent of ascorbate concentration (33). If ascorbate binds last, after O<sub>2</sub>, then at higher ascorbate concentration the reaction will be fully committed, because high ascorbate concentration prevents the release of O<sub>2</sub> and its equilibration with excess O<sub>2</sub>. A large forward commitment factor translates into an observed <sup>18</sup>O KIE of 1.0 (33), and lowering the ascorbate concentration will increase the measured <sup>18</sup>O KIE.

In contrast to the predicted effect, the measurements reveal that the <sup>18</sup>O KIE decreases from 1.0215 ± 0.0005 at saturating ascorbate concentration (20 mM) to 1.0157 ± 0.0004 at low ascorbate (2 mM, Fig. 4B), which suggests that another step becomes rate-limiting such that a smaller change in the oxygen bond order has been measured. Additionally, <sup>D2O</sup>*k*<sub>cat</sub>/*K*<sub>m</sub>(O<sub>2</sub>) decreases from 5.0 ± 0.9 (at 20 mM ascorbate) to 2.7 ± 0.7 (at 2 mM ascorbate), a value within experimental error of the background SIEs for the other kinetic parameters. The reduction of both <sup>18</sup>O KIE and <sup>D2O</sup>*k*<sub>cat</sub>/*K*<sub>m</sub>(O<sub>2</sub>) is attributed to a partially rate-determining binding of ascorbate at the reduced ascorbate concentrations. In an earlier study (13), the possibility of an effector site for ascorbate was postulated. In light of the proposal of very tight binding of ascorbate to such a site (13), this explanation does not appear relevant to the conditions of the present experiments (2 and 20 mM ascorbate). Further, since the kinetic properties of ACCO can accommodate the available data, there is no need to invoke the presence of an additional ascorbate binding site.

**Proposed Mechanism for O<sub>2</sub> Activation.** Considering all experimental observations, a mechanism for O<sub>2</sub> activation by ACCO is proposed (Fig. 5). Our working model is that, although an ordered mechanism is still in place for substrate and O<sub>2</sub>, ascorbate interaction with enzyme occurs in a random manner, depending on its concentration. At high, saturating concentrations, ascorbate is proposed to bind first, followed by ACC and O<sub>2</sub>. For such a kinetic mechanism, the fully rate-limiting step for *k*<sub>cat</sub>/*K*<sub>m</sub>(O<sub>2</sub>) is proposed to be the formation of an Fe<sup>IV</sup>=O species in a process that involves a PCET, consistent with the large <sup>18</sup>O KIE and <sup>D2O</sup>*k*<sub>cat</sub>/*K*<sub>m</sub>(O<sub>2</sub>). The oxidation of the Fe<sup>III</sup>—O<sub>2</sub><sup>•−</sup> species to Fe<sup>III</sup>—OOH by ascorbate is proposed to be reversible, similar to the reversible O<sub>2</sub> binding observed in hemerythrin (21). When the ascorbate concentration is below its *K*<sub>m</sub> value, ascorbate is proposed to bind last, subsequent to O<sub>2</sub>, with the actual binding being partially rate-limiting. Because ascorbate binding most probably does not involve a change in the oxygen bond order or a direct proton transfer, a reduction in both <sup>18</sup>O KIE and SIE values is expected, as observed experimentally. These findings suggest

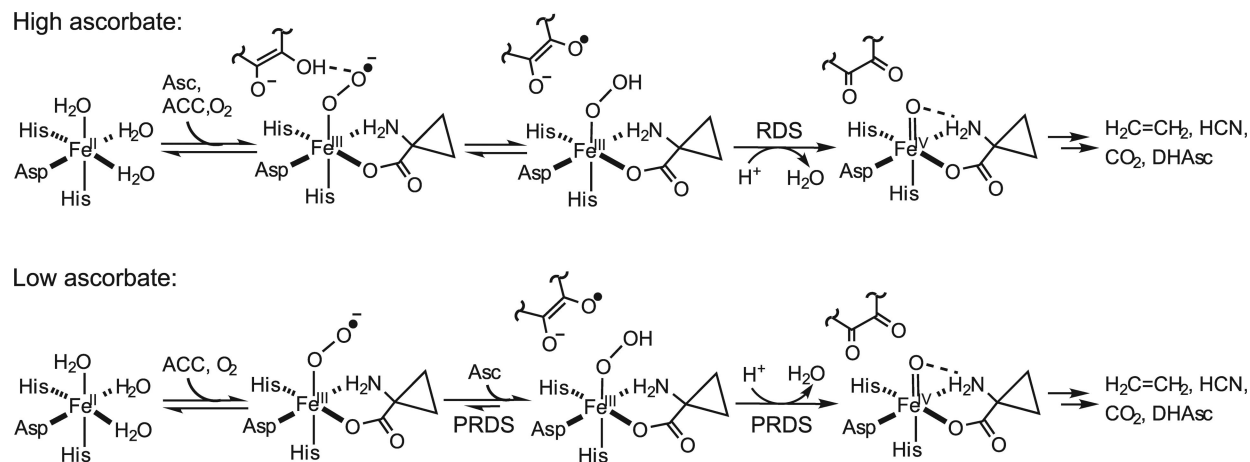


**Fig. 5.** Mechanisms for  $O_2$  activation in ACCO involving ascorbate-dependent formation of the  $Fe^{IV}=O$  species. Only the redox-active fragment of ascorbate is shown. Asc, ascorbate; DHAsc, dehydroascorbate; RDS, rate-determining step; PRDS, partially rate-determining steps.

that, unlike substrate, which directly coordinates to the iron center, binding of ascorbate at the active site of ACCO is not an essential step for the conversion of the metal center from six- to five-coordinate and initial reduction of  $O_2$  to form the  $Fe^{III}-O_2^-$  species. Although it is possible that product release or the reduction of  $Fe(III)$  to  $Fe(II)$  may be rate-limiting under certain conditions (13), the rate-limiting step on  $k_{cat}/K_m(O_2)$  is unlikely to depend on these steps. Because the ascorbate concentration has a pronounced effect on  $^{18}O$  KIE and on  $D_2O k_{cat}/K_m(O_2)$ , it becomes clear that under catalytic conditions high ascorbate concentrations facilitate the rapid formation of the active oxidant.

In summary, several insights have been obtained about the mechanism of  $O_2$  activation by the nonheme iron enzyme ACCO. SIEs and competitive  $^{18}O$  KIEs reveal a detailed picture of the  $Fe/O_2$  intermediates formed during  $O_2$  activation. The presence of a large  $D_2O k_{cat}/K_m(O_2)$  suggests that  $O_2$  activation involves a PCET (or HAT), although the source of proton cannot be unambiguously determined. The elevated  $^{18}O$  KIE value for ACCO, which is independent of solvent deuteration, strongly supports the formation of an  $Fe^{IV}=O$  intermediate in the rate-determining step of  $O_2$  activation; this species thus is implicated as the oxidant responsible for subsequent substrate activation. Based on the data herein, the slow single-turnover reaction reported for ACCO in the absence of ascorbate (13) is attributed to an alternate, non-catalytic pathway involving electron transfer from another molecule of ACCO. These studies make ACCO a unique system, providing kinetic as opposed to the more conventional spectroscopic evidence (14–17) for the presence of an  $Fe^{IV}=O$  species. It is important to mention that, to our knowledge,  $^{18}O$  KIE measurements have not been performed before for an  $O_2$ -activating, nonheme iron enzyme. Although  $^{18}O$  KIEs were reported for the pterin-dependent tyrosine hydroxylase, in that case, the initial  $O_2$  activation is proposed to occur at the pterin cofactor and not at the iron center (34). Additionally, the role of ascorbate on  $O_2$  activation has been investigated, leading to a kinetic model in which ascorbate binds to enzyme in a random manner. Thus, although ascorbate is required for rapid  $Fe^{IV}=O$  formation under catalytic turnover, the presence of this reductant is not required for initial  $O_2$  binding (13).

Several recent studies have used  $^{18}O$  KIEs to probe the steps involved in  $O_2$  reduction and to reveal the nature of the metal/ $O_2$  intermediate formed in the first irreversible step of enzymatic reactions (22, 25). This technique emerges as a

valuable companion to pre-steady-state kinetic analyses, which investigate the nature of the intermediate immediately preceding the rate-determining step. We are presently employing stopped-flow methods to monitor the intermediate that precedes the formation of the postulated  $Fe^{IV}=O$  species in ACCO. From this study, the observed  $^{18}O$  KIE is available as a standard for other enzymatic or model systems proposed to involve similar  $Fe/O_2$  intermediates. The results reported herein open up the opportunity for similar measurements on a range of  $\alpha$ KG-dependent and other nonheme iron enzymes.

## Materials and Methods

**General.** All reagents were purchased from commercial sources and used without further purification unless otherwise indicated.

**Overexpression and Purification of ACCO.** ACCO from *Lycopersicon esculentum* (ACO1) was produced in *Escherichia coli* strain BL21(DE3)pLysS and purified by a two-column purification procedure as previously described (12).

**Steady-State Kinetics.** Initial velocities were measured by the rate of oxygen consumption at 25°C, pH 7.2, using a Yellow Springs Instrument biological oxygen monitor (model 5300) as previously described (12). Temperature was maintained at  $25 \pm 0.1^\circ C$  with a Neslab circulating water bath. Standard reaction mixture (1 ml) contained 100 mM MOPS, pH 7.2, 20 mM  $NaHCO_3$ , 100 mM NaCl, and various amounts of ascorbate and ACC. When ACC and ascorbate were kept constant, concentrations were maintained at 1 and 20 mM, respectively. When the oxygen concentration was varied, the reaction mixture was equilibrated by stirring for at least 10 min with the appropriate premixed  $O_2/N_2$  gas mixture to obtain the desired oxygen concentration. Starting oxygen concentrations were determined by using the oxygen monitor that was calibrated with air-saturated water (258  $\mu M$  oxygen at 25°C). Reactions were initiated with 2  $\mu l$  of ACCO reconstituted with equimolar  $Fe(NH_4)_2(SO_4)_2$ . Because of the loss of activity on prolonged exposure to  $Fe(II)$  in the presence of oxygen (35, 36), ACCO was reconstituted in small aliquots and used within 30 min. Concentration of ACCO is as indicated in figure legends. All initial rates were measured under conditions where  $<5\%$  of any given substrate was consumed. All rates were calculated subtracting background oxygen consumption attributable to ascorbate and/or  $Fe(II)$  in the absence of enzyme. Data from initial velocity experiments with varying substrate concentrations were fitted to the Michaelis–Menten equation by using the program KaleidaGraph. The kinetic parameters are reported with errors of  $\pm 1\sigma$ .

**SIEs on Steady-State Parameters.** Initial rates were measured as described above. The standard buffer was prepared in  $D_2O$  (99.9%) by dissolving MOPS,  $NaHCO_3$ , and NaCl in  $D_2O$  and then titrating to pH 7.2 with a KOD solution. A value of 0.4 was added to the reading on the pH meter to correct to pH (37). To avoid  $H_2O$  contamination in the  $D_2O$  reactions, the electrode tip was soaked in  $D_2O$  before each reaction. In parallel, a buffer was prepared in  $H_2O$

for direct comparison. SIEs are reported with errors obtained by using appropriate error propagation methods.

**$^{18}\text{O}$  KIEs.**  $^{18}\text{O}$  KIEs were measured competitively as described in refs. 21 and 26. Reactions were carried out in 100 mM MOPS, pH 7.2, 20 mM  $\text{NaHCO}_3$ , 100 mM NaCl, and 2 mM or 20 mM sodium ascorbate at 25°C with 0.3–0.5 mM  $\text{O}_2$  and 3 mM ACC. The enzymatic reactions were initiated with a preincubated mixture of  $\text{ACCO:Fe}(\text{NH}_4)_2(\text{SO}_4)_2$  in a 1.75:1 ratio to minimize free iron in solution. Final concentrations typically were 3.5–8  $\mu\text{M}$  ACCO and 2–4  $\mu\text{M}$  Fe. Reactions were carried out in  $\text{D}_2\text{O}$  under similar conditions, the buffer being prepared as described above. The amount of  $\text{O}_2$  consumed was corrected for the background  $\text{O}_2$  consumption attributed to ascorbate and Fe in absence of enzyme. In all experiments, the  $\text{O}_2$  consumed in nonenzymatic reactions accounted for <10% of the total  $\text{O}_2$  consumed. The  $^{18}\text{O}$  KIE also was measured for the background oxygen consumption (at 1  $\mu\text{M}$  Fe), for comparison with the enzymatic reaction. The  $^{18}\text{O}/^{16}\text{O}$  ratios were measured by using isotopic ratio mass spectrometry (Laboratory for Environmental and Sedimentary Geochemistry, Department of Earth and Planetary Science, University of California, Berkeley, CA). The  $^{18}\text{O}$  KIEs were

obtained by fitting the  $^{18}\text{O}/^{16}\text{O}$  ratio of ratios versus fractional conversion according to Eq. 1. All KIEs are reported with errors of  $\pm 1\sigma$  from the nonlinear regression fit to Eq. 1.

**Calculation of  $^{18}\text{O}$  EIEs.** The EIEs can be expressed as a product of three terms, contributed from the zero-point energies (ZPE), excited vibration states (EXC), and the mass and moments of inertia (MMI):  $\text{EIE} = \text{ZPE} \times \text{EXC} \times \text{MMI}$  (28). All three terms are related to vibrational frequencies of  $^{18}\text{O}$ - and  $^{16}\text{O}$ -containing reactants and products, as described in ref. 21. The measured frequency of 821  $\text{cm}^{-1}$  ( $\Delta^{18}\text{O} = 34 \text{ cm}^{-1}$ ) for the  $\text{Fe}^{\text{IV}}=\text{O}$  intermediate in TauD was used for calculation of the  $^{18}\text{O}$  EIE (17). For the model reaction (Table 2, entry 3), the  $^{18}\text{O}$  label can end up in either  $\text{Fe}^{\text{IV}}=\text{O}$  or  $\text{H}_2\text{O}$ . The populations of the two isotopic distributions are expected to be close to each other; hence, the  $^{18}\text{O}$  EIE was calculated by using the formula:  $^{18}\text{EIE}_{\text{calc}} = 2 / (^{18,16}\kappa^{-1} + ^{16,18}\kappa^{-1})$  (21).

**ACKNOWLEDGMENTS.** We thank Dr. Wenbo Yang for measurement of the  $^{18}\text{O}/^{16}\text{O}$  ratios at the Laboratory for Environmental and Sedimentary Geochemistry, University of California, Berkeley. This work was supported by National Institutes of Health Grant GM 25765 (to J.P.K.) and National Research Service Award Postdoctoral Fellowship F32GM 078802-01 (to L.M.M.).

- John P (1997) Ethylene biosynthesis: The role of 1-aminocyclopropane-1-carboxylate (ACC) oxidase, and its possible evolutionary origin. *Physiol Plant* 100:583–592.
- Adams DO, Yang SF (1979) Ethylene biosynthesis: Identification of 1-aminocyclopropane-1-carboxylic acid as an intermediate in the conversion of methionine to ethylene. *Proc Natl Acad Sci USA* 76:170–174.
- Dong JG, Fernández-Maculec JC, Yang SF (1992) Purification and characterization of 1-aminocyclopropane-1-carboxylate oxidase from apple fruit. *Proc Natl Acad Sci USA* 89:9789–9793.
- Costas M, Mehn MP, Jensen MP, Que L, Jr (2004) Dioxygen activation at mononuclear nonheme iron active sites: Enzymes, models, and intermediates. *Chem Rev* 104:939–986.
- Fernández-Maculec JC, Dong JG, Yang SF (1993) Activation of 1-aminocyclopropane-1-carboxylate oxidase by carbon dioxide. *Biochem Biophys Res Commun* 193:1168–1173.
- Zhang ZH, Ren JS, Clifton IJ, Schofield CJ (2004) Crystal structure and mechanistic implications of 1-aminocyclopropane-1-carboxylic acid oxidase—The ethylene-forming enzyme. *Chem Biol* 11:1383–1394.
- Shaw JF, Chou YS, Chang RC, Yang SF (1996) Characterization of the ferrous ion binding sites of apple 1-aminocyclopropane-1-carboxylate oxidase by site-directed mutagenesis. *Biochem Biophys Res Commun* 225:697–700.
- Roach PL, et al. (1995) Crystal-structure of isopenicillin N synthase is the first from a new structural family of enzymes. *Nature* 375:700–704.
- Roach PL, et al. (1997) Structure of isopenicillin N synthase complexed with substrate and the mechanism of penicillin formation. *Nature* 387:827–830.
- Rocklin AM, et al. (1999) Role of the nonheme Fe(II) center in the biosynthesis of the plant hormone ethylene. *Proc Natl Acad Sci USA* 96:7905–7909.
- Brunhuber NMW, Mort JL, Christoffersen RE, Reich NO (2000) Steady-state kinetic mechanism of recombinant avocado ACC oxidase: Initial velocity and inhibitor studies. *Biochemistry* 39:10730–10738.
- Thrower JS, Blalock R, Klinman JP (2001) Steady-state kinetics of substrate binding and iron release in tomato ACC oxidase. *Biochemistry* 40:9717–9724.
- Rocklin AM, Kato K, Liu HW, Que L, Jr, Lipscomb JD (2004) Mechanistic studies of 1-aminocyclopropane-1-carboxylic acid oxidase: Single turnover reaction. *J Biol Inorg Chem* 9:171–182.
- Price JC, Barr EW, Glass TE, Krebs C, Bollinger JM (2003) Evidence for hydrogen abstraction from C1 of taurine by the high-spin Fe(IV) intermediate detected during oxygen activation by taurine: $\alpha$ -ketoglutarate dioxygenase (TauD). *J Am Chem Soc* 125:13008–13009.
- Price JC, Barr EW, Tirupati B, Bollinger JM, Krebs C (2003) The first direct characterization of a high-valent iron intermediate in the reaction of  $\alpha$ -ketoglutarate-dependent dioxygenase: A high-spin Fe(IV) complex in taurine: $\alpha$ -ketoglutarate dioxygenase (TauD) from *Escherichia coli*. *Biochemistry* 42:7497–7508.
- Price JC, Barr EW, Hoffart LM, Krebs C, Bollinger JM (2005) Kinetic dissection of the catalytic mechanism of taurine: $\alpha$ -ketoglutarate dioxygenase (TauD) from *Escherichia coli*. *Biochemistry* 44:8138–8147.
- Proshlyakov DA, Henshaw TF, Monterosso GR, Ryle MJ, Hausinger RP (2004) Direct detection of oxygen intermediates in the non-heme Fe enzyme taurine: $\alpha$ -ketoglutarate dioxygenase. *J Am Chem Soc* 126:1022–1023.
- Tierney DL, Rocklin AM, Lipscomb JD, Que L, Jr, Hoffman BM (2005) ENDOR studies of the ligation and structure of the non-heme iron site in ACC oxidase. *J Am Chem Soc* 127:7005–7013.
- Zhou J, Rocklin AM, Lipscomb JD, Que L, Jr, Solomon EI (2002) Spectroscopic studies of 1-aminocyclopropane-1-carboxylic acid oxidase: Molecular mechanism and  $\text{CO}_2$  activation in the biosynthesis of ethylene. *J Am Chem Soc* 124:4602–4609.
- Thrower JS, Mirica LM, Mccusker KP, Klinman JP (2006) Mechanistic investigations of 1-aminocyclopropane 1-carboxylic acid oxidase with alternate cyclic and acyclic substrates. *Biochemistry* 45:13108–13117.
- Tian GC, Klinman JP (1993) Discrimination between O-16 and O-18 in oxygen-binding to the reversible oxygen carriers hemoglobin, myoglobin, hemerythrin, and hemocyanin—A new probe for oxygen-binding and reductive activation by proteins. *J Am Chem Soc* 115:8891–8897.
- Roth JP, Klinman JP (2004) Oxygen-18 isotope effects as a probe of enzymatic activation of molecular oxygen in *Isotopes Effects in Chemistry and Biology*, ed Limbach H-H (Marcel Dekker, New York), pp 645–669.
- Pirrung MC (1999) Ethylene biosynthesis from 1-aminocyclopropanecarboxylic acid. *Acc Chem Res* 32:711–718.
- Quinn DM (2004) Theory and practice of solvent isotope effects in *Isotopes Effects in Chemistry and Biology*, ed Limbach H-H (Marcel Dekker, New York), pp 995–1018.
- Roth JP (2007) Advances in studying bioinorganic reaction mechanisms: Isotopic probes of activated oxygen intermediates in metalloenzymes *Curr Opin Chem Biol* 11:142–150.
- Tian GC, Berry JA, Klinman JP (1994) O-18 kinetic isotope effects in the dopamine  $\beta$ -monooxygenase reaction—Evidence for a new chemical mechanism in nonheme metallomonooxygenases. *Biochemistry* 33:226–234.
- Francisco WA, Blackburn NJ, Klinman JP (2003) Oxygen and hydrogen isotope effects in an active site tyrosine to phenylalanine mutant of peptidylglycine  $\alpha$ -hydroxylating monooxygenase: Mechanistic implications. *Biochemistry* 42:1813–1819.
- Bigeleisen J, Mayer MG (1947) Calculation of equilibrium constants for isotopic exchange reactions. *J Chem Phys* 15:261–267.
- Burger RM, Tian GC, Drlca K (1995) Oxygen isotope effect on activated bleomycin stability. *J Am Chem Soc* 117:1167–1168.
- Bigeleisen J, Wolfsberg M (1958) Theoretical and experimental aspects of isotope effects in chemical kinetics. *Adv Chem Phys* 1:15–76.
- Lanci MP, Brinkley DW, Stone KL, Smirnov VV, Roth JP (2005) Structures of transition states in metal-mediated  $\text{O}_2$ -activation reactions. *Angew Chem Int Ed* 44:7273–7276.
- Mirica LM, Ottenwaelder X, Stack TDP (2004) Structure and spectroscopy of copper-dioxygen complexes. *Chem Rev* 104:1013–1045.
- Cook PF, Cleland WW (1981) Mechanistic deductions from isotope effects in multireactant enzyme mechanisms. *Biochemistry* 20:1790–1796.
- Francisco WA, Tian GC, Fitzpatrick RF, Klinman JP (1998) Oxygen-18 kinetic isotope effect studies of the tyrosine hydroxylase reaction: Evidence of rate limiting oxygen activation. *J Am Chem Soc* 120:4057–4062.
- Barlow JN, Zhang ZH, John P, Baldwin JE, Schofield CJ (1997) Inactivation of 1-aminocyclopropane-1-carboxylate oxidase involves oxidative modifications. *Biochemistry* 36:3563–3569.
- Zhang ZH, Barlow JN, Baldwin JE, Schofield CJ (1997) Metal-catalyzed oxidation and mutagenesis studies on the iron(II) binding site of 1-aminocyclopropane-1-carboxylate oxidase. *Biochemistry* 36:15999–16007.
- Schowen KB, Schowen RL (1982) Solvent isotope effects on enzyme systems. *Methods Enzymol* 87:551–606.